New isospin effects in central heavy-ion collisions at Fermi energies

F. Gagnon-Moisan,[1,2,*] E. Galichet,[1,3] M.-F. Rivet,[1,†] B. Borderie,[1] M. Colonna,[4] R. Roy,[2] G. Ademard,[1,5] M. Boisjoli,[2,5] E. Bonnet,[5] R. Bougault,[6] A. Chbihi,[5] J. D. Frankland,[5] D. Guinet,[7] P. Lautesse,[7,‡] E. Legouée,[6] N. Le Neindre,[6] L. Manduci,[5,8] P. Marini,[5] P. Napolitani,[1] M. Pârlog,[6,9] P. Pawłowski,[10] E. Rosato,[11] and M. Vigilante[11]
(INDRA Collaboration)[§]

[1]*Institut de Physique Nucléaire, CNRS-IN2P3 and Université Paris-Sud 11, F-91406 Orsay, France*
[2]*Université Laval, Québec, G1V 0A6 Canada*
[3]*Conservatoire National des Arts et Métiers, F-75141 Paris Cedex 03, France*
[4]*Laboratori Nazionali del Sud-Istituto Nazionale Fisica Nucleare, I-95123 Catania, Italy*
[5]*GANIL, CEA-DSM/CNRS-IN2P3, F-14076 Caen Cedex, France*
[6]*LPC Caen, ENSICAEN, Université de Caen, CNRS-IN2P3, F-14050 Caen Cedex, France*
[7]*Institut de Physique Nucléaire, UCBL, Université de Lyon, CNRS-IN2P3, F-69622 Villeurbanne Cedex, France*
[8]*EAMEA, CC19 50115 Cherbourg-Octeville Cedex, France*
[9]*National Institute for Physics and Nuclear Engineering, RO-76900 Bucharest-Măgurele, Romania*
[10]*IFJ-PAN, 31-342 Kraków, Poland*
[11]*Dipartimento di Scienze Fisiche e Sezione INFN, Università di Napoli "Federico II", I-80126 Napoli, Italy*
(Received 25 July 2012; published 16 October 2012)

Isospin effects on multifragmentation properties were studied thanks to nuclear collisions between different isotopes of xenon beams and tin targets. It is shown that, in central collisions leading to multifragmentation, the mean number of fragments and their mean kinetic energy increase with the neutron-richness of the total system. Comparisons with a stochastic transport model allow to attribute the multiplicity increase to the multifragmentation stage, before secondary decay. The total charge bound in fragments is proposed as an alternate variable to quantify preequilibrium emission and to investigate symmetry energy effects.

DOI: 10.1103/PhysRevC.86.044617 PACS number(s): 25.70.Pq, 24.10.−i

I. INTRODUCTION

One of the present motivations for investigating heavy-ion collisions at intermediate energy is the improvement of the knowledge of the equation of state (EOS) for nuclear matter. More specifically the formulation of an adequate symmetry term is required to progress, and the density dependence of this term both at subnormal and supranormal densities is still debated. Further experimental constraints are clearly necessary. Within the next decade physicists expect the advent of new heavy-ion accelerators, providing high-intensity exotic beams, in order to study reactions covering a broad range of isospin (N/Z) ratios; in the meantime information on isospin effects can be obtained thanks to a judicious choice of projectile-target couples. Comparisons of several calculated and experimentally measured isospin-dependent variables already provided some hints on the symmetry term, but the results are still highly model and experiment dependent [1–7].

In this line the INDRA Collaboration has studied collisions between ^{124,136}Xe projectiles, with an incoming energy of 32 and 45 A MeV, and ^{112,124}Sn targets. We show in this paper that, in central collisions, the mean charged-product and fragment $(Z \geqslant 5)$ multiplicities, and mean fragment kinetic energies, depend on the isospin of the total system. The commonly accepted reaction scenario for central heavy-ion collisions around the Fermi energy, validated by stochastic transport models, is the following [8]: there is first a compression phase, the strength of which depends on the masses and mass asymmetry of the incident partners. This stage is followed by an expansion phase accompanied by the emission of fast preequilibrium particles. The diluted system enters the spinodal region of the phase diagram and eventually breaks into several excited fragments, light particles, and nucleons (multifragmentation); when the configuration is frozen, namely when the nuclear interaction between fragments becomes negligible, one speaks of the "freeze-out" stage. Finally the charged products move apart, further accelerated by the Coulomb force, while losing their excitation energy through evaporation.

In this framework we shall test, through comparisons with a stochastic transport model, the origin of the isospin dependence observed for the aforementioned variables.

II. EXPERIMENT

Beams of 32 and 45 A MeV ^{124,136}Xe accelerated by the Grand Accélérateur National d'Ions Lourds (GANIL) impinged on 530 μg cm^{-2} ^{112,124}Sn targets. Beam intensity was about 3–5 $\times$ 10^7 particles per second to avoid event pile-up. Charged products were detected and identified with the 4π INDRA array [9], which comprises 336 two- or three-member telescopes arranged in a cylindrical geometry around the beam axis. The array was upgraded as follows [10]: twelve 300-μm silicon, 14-cm CsI(Tl) telescopes replaced the

*Current address: PTB Brauncshweig, Bundesallee 100, 38116 Braunschweig, Germany.
†rivet@ipno.in2p3.fr
‡Current address: S2HEP (EA4148), UCBL/ENSL, Université de Lyon, Villeurbanne, France.
§http://indra.in2p3.fr/spip/

TABLE I. Available systems and measured cross sections. Systematic errors on cross sections are estimated to 15%

Projectile	Target	N/Z syst.	$E_{\text{proj.}}$ (A MeV)	σ (b)	$E_{\text{proj.}}$ (A MeV)	σ (b)
^{124}Xe	^{112}Sn	1.269	32	5.16	45	4.73
^{124}Xe	^{124}Sn	1.385	32	5.14		
^{136}Xe	^{112}Sn	1.385	32	5.90	45	
^{136}Xe	^{124}Sn	1.50	32	5.81	45	5.02

phoswiches of the first ring, and seven of the 300-μm silicon wafers were replaced by 150-μm wafers, with an increased amplifier gain, in order to identify isotopes up to nitrogen. In the standard silicon-CsI(Tl) telescopes (2°–45°) elements were identified within one charge unit; in addition between 14° and 45° these telescopes provided isotopic identification up to carbon. The same Z resolution was obtained in the first-stage ionization-chamber silicon or ionization-chamber CsI(Tl) telescopes up to $Z = 20$. For low-energy heavier nuclei, Z are known with an uncertainty of 1–2 charge units [11]. In this paper, the term "fragments" refers to charged products with a charge $Z \geqslant 5$ whereas light charged particles (lcp) stands for particles with a charge $Z \leqslant 2$.

Most of data taking was done with an online trigger requiring at least four fired INDRA telescopes. For a better overview of the reactions, some inclusive measurements (one telescope fired) were also performed.

Absolute cross sections were derived from the measured target thicknesses, the counting of ions collected in the Faraday cup located at the end of the beam line, and the acquisition dead time. The charge of ions reaching the cup was obtained using the formulas of Ref. [12]. The error on cross sections is estimated to be 15%, while relative errors between two systems are lower, around 3%.

Table I summarizes the studied systems and the isospin contents of the total systems. Note that two of the systems have the same N/Z, allowing us to study entrance channel mass-asymmetry effects. We also indicate the measured inclusive cross sections (trigger multiplicity $\geqslant$1). In the offline analysis we required at least one identified charged product and rejected events formed of a single charged product with an atomic number close to the projectile one, in order to exclude elastic scattering. The cross sections so obtained are close to the reaction cross sections calculated with the systematics of Kox [13] at 32 A MeV whereas they are smaller by about 1 b at 45 A MeV.

Figure 1 shows the charged-product multiplicity distributions of identified nuclei at 32 A MeV, for data with an online trigger multiplicity $M \geqslant$1. For low multiplicities the cross sections are higher for the neutron-rich system; the trend is reversed for multiplicities larger than 20, and the distribution extends to higher values for the neutron-poor system. The two systems ^{124}Xe + ^{124}Sn and ^{136}Xe + ^{112}Sn display intermediate values. A first isospin effect appears already on raw variables: higher charged product multiplicities are observed when the system contains fewer neutrons; it is indeed expected that a neutron-rich system will preferentially emit neutrons to the detriment of light charged particles, which dominate in the charged product multiplicity.

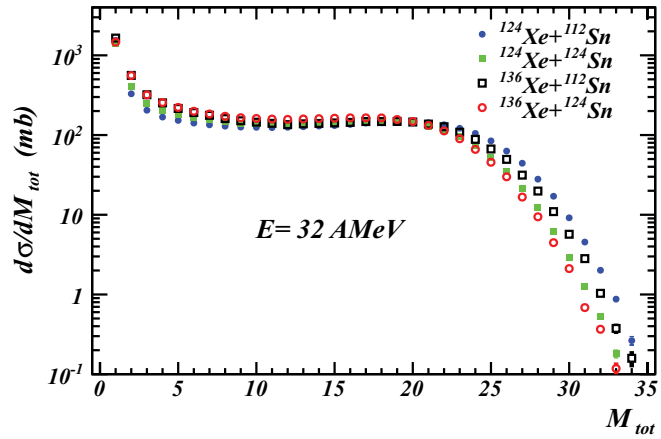

FIG. 1. (Color online) Charged-product multiplicity distributions for the different systems at 32 A MeV. Error bars are statistical.

III. COMPACT SHAPE EVENTS FROM CENTRAL COLLISIONS

In the following we shall report on data obtained with an online trigger $M \geqslant 4$ for which we obtained very high statistics. As in previous studies [14–17] we select quasicomplete events by requiring that the sum of the charges of the detected products, Z_{tot}, be at least equal to 80. Due to the response of INDRA to the kinematics of quasisymmetric collisions such as Xe+Sn, this choice favors *de facto* central collisions. We then isolate compact shape events (quasifusion) through the additional condition that the flow angle (θ_{flow}) be greater than 60°. Let us recall that θ_{flow} characterizes the main direction of matter emission in the reaction center of mass and is determined by the kinetic energy flow tensor calculated from fragment momenta. More than 10^5 events were selected in all cases, corresponding to measured cross sections of 30–40 mb at 32 A MeV, and 20–25 mb at 45 A MeV. These values are slightly larger than those previously measured for the ^{129}Xe + $^{\text{nat}}$Sn system [16]. The total cross section for quasifusion, taking into account detection efficiency and selection biases, is estimated to reach ∼200–250 mb at 32 A MeV, and ∼170 mb at 45 A MeV (the difference between estimated and measured cross sections is due to the limits on θ_{flow} and on Z_{tot} imposed in the selection, which cut some of events that can be attributed to the quasifusion mechanism [18]).

A. Multiplicities

Table II displays the different average multiplicities measured for the selected class of events, for all studied systems: M_{tot} is the total charged product multiplicity, and M_{lcp} and M_{frag} refer to the light charged particle and fragment multiplicities, which are shown in Fig. 2. Results from the reaction ^{129}Xe + $^{\text{nat}}$Sn have been added [16]: the composite system is the same as that formed by ^{136}Xe + ^{112}Sn and ^{124}Xe + ^{124}Sn (the average mass number of $^{\text{nat}}$Sn is 119). As in the unsorted data, at each beam energy the average multiplicities of charged products and of light charged particles decrease for increasing N/Z of the total system. Conversely

TABLE II. Average measured multiplicities of charged products, M_{tot}, of light charged particles (H, He), M_{lcp}, and of fragments, M_{frag} for the different systems studied. Number in parentheses are the standard deviations of the corresponding distributions. Statistical errors on mean values are smaller than 0.01 for M_{tot} and M_{lcp} and M_{frag}. Results on line 3 are from Ref. [16].

System	$E/A = 32$ MeV			$E/A = 45$ MeV		
	$\langle M_{tot}\rangle$	$\langle M_{lcp}\rangle$	$\langle M_{frag}\rangle$	$\langle M_{tot}\rangle$	$\langle M_{lcp}\rangle$	$\langle M_{frag}\rangle$
^{124}Xe + ^{112}Sn	25.12 (2.90)	19.66 (3.24)	4.11 (1.16)	32.65 (3.24)	25.96 (3.68)	4.30 (1.18)
^{124}Xe + ^{124}Sn	23.71 (2.88)	18.06 (3.22)	4.23 (1.17)			
^{129}Xe + ^{nat}Sn	23.92 (3.00)	18.37 (3.28)	4.13 (1.17)	31.4 (3.21)	24.57 (3.64)	4.39 (1.20)
^{136}Xe + ^{112}Sn	24.23 (3.01)	18.38 (3.30)	4.36 (1.18)	31.04 (3.28)	24.02 (3.67)	4.52 (1.20)
^{136}Xe + ^{124}Sn	23.07 (3.00)	16.97 (3.28)	4.54 (1.20)	30.0 (3.26)	22.68 (3.66)	4.71 (1.23)

the fragment multiplicity increases. The three systems with the same N/Z show very close mean lcp multiplicity values, which indicates that the entrance channel mass asymmetry has a small influence. The same is not true for mean fragment multiplicities, whereas their standard deviations are equal. While we may suspect some difference in the INDRA response between the present data and those of Ref. [16], such an explanation does not hold for ^{124}Xe + ^{124}Sn and ^{136}Xe + ^{112}Sn at 32 A MeV. In that case we might envisage some physical reason, which requires further investigation. Previous studies [19,20] already indicated that more fragments are emitted for neutron-rich systems. The available energy per nucleon, at the same incident energy, is the same for all systems, within 1%, so the increased number of fragments cannot be explained by a larger available energy. Moreover M_{frag} modestly increases between 32 and 45 A MeV: it was indeed shown in Ref. [16] that for the system ^{129}Xe + ^{nat}Sn M_{frag} presents a maximum for an incident energy around 40 A MeV.

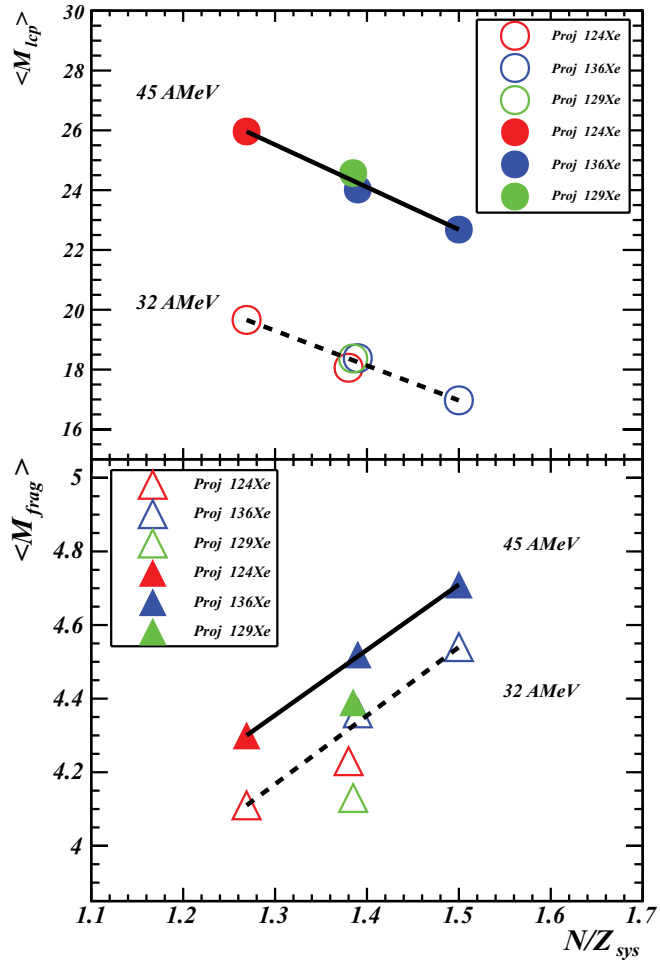

FIG. 2. (Color online) Evolution of the light charged particle and fragment multiplicities versus the N/Z of the total systems, at the two energies. Error bars are smaller than the size of the symbols.

In previous works the difference in fragment multiplicities was attributed to phase-space effects [20], because statistical calculations (expanding-evaporating source model [21]) reproduce the observation, or to sequential decay effects [19]. In the present data the fragment multiplicity increases by 10%, both at 32 and 45 A MeV, between the lightest and the heaviest systems. This corresponds to the mass increase between these systems, which may recall the scaling law observed in Ref. [22], expected if multifragmentation originates from volume instabilities (spinodal decomposition). Using stochastic transport codes we can test whether the increased fragment multiplicity arises from the dynamical or from the secondary decay stage of the reaction.

B. Fragment kinetic energies

The average fragment kinetic energies (in the center of mass) provide another piece of information on possible isospin effects. Figure 3 displays this observable for the different systems at the two incident energies, excluding the largest fragment of each partition. The general aspect is the same as that previously observed for ^{129}Xe + ^{nat}Sn [15,17,23], namely an almost linear rise of the average energy when the atomic number increases. Conversely the mean energy of the largest fragment (see one example in Fig. 3) increases for small Z and then decreases. We confirm that, for a given Z, the mean energy is smaller when it corresponds to the largest fragment [17,23]. The average kinetic energy for a given element is slightly larger (by 2–3 MeV) at the higher incident energy.

The present data provide new information: at a given incident energy the mean fragment kinetic energy depends on the isospin of the system; the heavier the mass of the system, the larger the fragment kinetic energy is. We have verified that the nonmeasurement of the masses of the heavy fragments is not responsible for the observed effect. Indeed the mean measured kinetic energies, in the laboratory, are larger for the

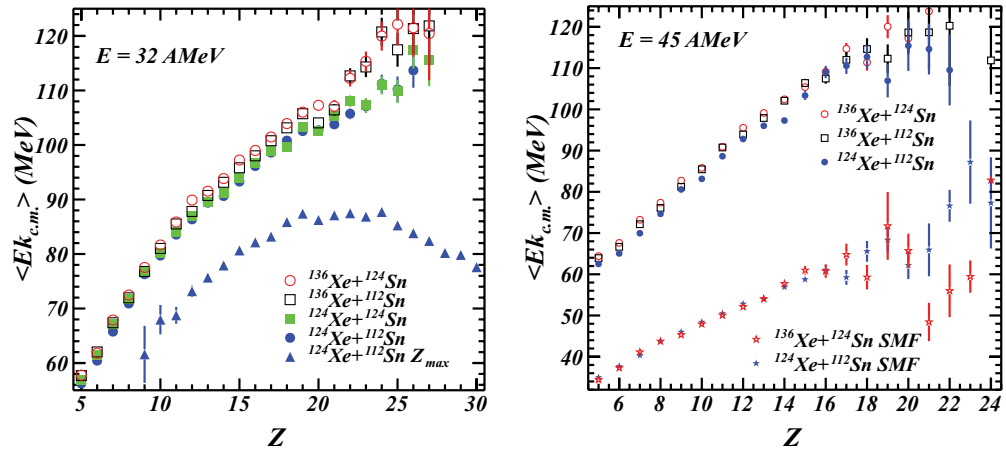

FIG. 3. (Color online) Average fragment kinetic energy, in the reaction center of mass, vs the fragment atomic number for the selected events at 32 (left) and 45 (right) A MeV. The largest fragment of each partition has been removed. The average kinetic energy of the largest fragment is displayed for $^{124}\mathrm{Xe} + {}^{112}\mathrm{Sn}$ at 32 A MeV. Open symbols denote ^{136}Xe projectiles, closed symbols denote ^{124}Xe projectiles. Circles, squares, and triangles: experimental data; stars: stochastic mean field (SMF) simulations (cold fragments, filtered).

neutron-rich system. The mean measured masses for $Z = 5$–8 are also larger.

The fragment kinetic energy is the superimposition of a disordered thermal motion and an ordered term. The former term comes from the temperature of the fragmenting system at freeze-out; the latter one, radially directed, originates from the Coulomb force, which depends on the system and fragment charges, and an expansion term proportional to the fragment mass [24–26]. At a given available energy the thermal term is expected to be identical for all systems. The same holds for the Coulomb term as the system charges remain very close even after preequilibrium emission (see next section). Moreover the increase of the fragment multiplicity with the system mass should slightly decrease the Coulomb part [27], which is not the observed effect. In this context, the increase of the fragment kinetic energy signals the larger masses of the primary fragments when the system initially contains more neutrons. This is true if the expansion energy per nucleon does not depend on the initial isospin of the system, at a given incident energy. Isospin differences between systems thus seem to survive preequilibrium emission [28].

IV. COMPARISON OF DATA WITH A STOCHASTIC MEAN FIELD MODEL

We used the stochastic mean field (SMF) calculation described in Ref. [29]. Simulations were performed for collisions corresponding to all systems (Table I), up to a time equal to 300 fm/c. The isoscalar EOS is soft ($K_\infty = 200$ MeV), and two parametrizations of the potential part of the symmetry energy are used [30], an asystiff one linearly increasing with density while the asysoft form (SKM*) has a maximum around normal density. The collision term uses the free nucleon-nucleon cross section, with its isospin, energy and angular dependences.[1] This version of the model is the same as the one used in Ref. [30], in which information on the asy-stiffness of the EOS was derived from isospin diffusion in the Ni+Au system at 52 and 74 A MeV. There is a great interest in finding additional experimental constraints on the density dependence of the symmetry energy in the same theoretical framework.

At 45 A MeV we observe the formation of a single source which subsequently breaks into several fragments. At 32 A MeV, conversely to the Brownian one-body (BOB) calculations [31] shown in Refs. [16,17,32], the systems do not multifragment in head-on collisions. However it should be noticed that while the BOB calculations were perfomed for a thermalized source mimicking the composite system at the moment of maximum compression, here the whole dynamical evolution of the system, from the beginning of the reaction, is simulated by the SMF approach. Hence the impact of preequilibrium effects on the dynamics could be different in the two treatments.

Fragments are recognized by applying a coalescence procedure to the one-body density, connecting nearby cells in which the density is larger than a cutoff value, taken equal to $\rho_0/5$ ("liquid phase"). We have shown in Ref. [32] that, at 300 fm/c, the fragment multiplicity is independent of the exact value of the cutoff density. The remaining early emitted nucleons constitute the "gas phase." The fragment phase space configuration at 300 fm/c is injected in the SIMON code [33] which performs the secondary decay during the propagation of all products under the Coulomb field, thus preserving space-time correlations. Note that the fragment excitation energies at 300 fm/c (∼3.3 A MeV) agree well with experimental determinations [15,34]. One thousand events were run with SMF for each system, then each primary event was deexcited 20 times. The cold products were finally filtered through a geometrical replica of the INDRA array described in the code PANFORTE [35]. Because in the present calculations free nucleons ("gas phase") emitted along the dynamical evolution are not taken into account in the subsequent deexcitation and Coulomb propagation steps, the selection on the total detected

[1]With an upper limit of 50 mb, to suppress spurious low-energy collisions.

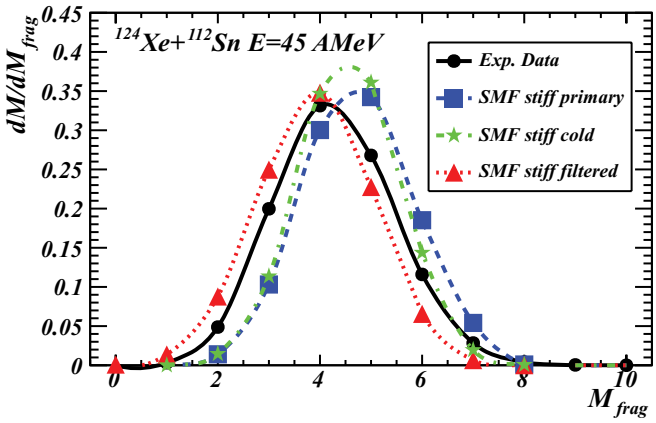

FIG. 4. (Color online) Fragment multiplicity distributions, normalised to the number of events, for ^{124}Xe + ^{112}Sn at 45 A MeV: experimental values (circles), primary fragments (squares), and cold fragments before (stars) and after (triangles) filtering. The asystiff EOS is used. Statistical errors are smaller than the symbol sizes.

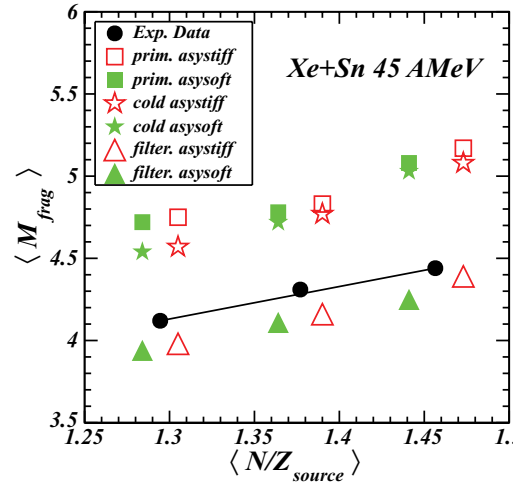

FIG. 5. (Color online) Average fragment multiplicities, for the different systems at 45 A MeV: experimental values (circles, the line is to guide the eye), calculated values for primary fragments (squares), and cold fragments before (stars) and after (triangles) filtering are plotted vs the source N/Z. Asystiff EOS: open symbols; asysoft EOS: filled symbols. In all cases statistical error bars are smaller than the symbol sizes.

charge cannot be used. Moreover only fragment properties can be compared to the experimental values.

A. Fragment multiplicities

We firstly verified the pertinence of the simulation by comparing calculated and measured distributions for some observables. We found that the charge distributions are reasonably reproduced [36]. We show in Fig. 4 an example of fragment multiplicity distributions: for the ^{124}Xe + ^{112}Sn at 45 A MeV the measured experimental distribution is plotted together with those of primary fragments, cold fragments, and the filtered distribution. The primary and cold fragment distributions are very similar, both the width and the average value of the latter being only slightly smaller than those of the former. Let us recall that we consider fragments starting from boron ($Z = 5$). Two reasons support this choice in the simulations: first, the yield of primary fragments is less sensitive to the fragment formation process, which comes from spinodal decomposition in the SMF model and strongly disfavors the formation of very small fragments [37]. Second, these fragments are essentially remnants of primary hot fragments, whereas final Li and Be isotopes are also populated by secondary decay.[2] The filtered distribution shows a good agreement with the experimental one.

The full set of data is represented in Fig. 5. Average multiplicity values are reported as a function of the N/Z of the sources, taken at $t = 120$ fm/c (see next subsection). The experimental points are located at the average N/Z of the asystiff and asysoft sources. We first observe that the multiplicity of primary fragments (squares) increases with the isospin of the multifragmenting source, which allows us to state that the experimental trend is essentially due to the preequilibrium stage of the collision. It would support the scaling law of multiplicity with system mass expected from a spinodal decomposition. The cooling of the fragments only slightly decreases the multiplicities; more so when the projectile is ^{124}Xe. Indeed, fragments from the less neutron-rich system are expected to evaporate more charged products, leading to more final fragments with a charge smaller than 5. Finally, for all systems the detection reduces the fragment multiplicity by about 0.6 units. These final calculated multiplicities are in good agreement with the experimental values. The figure also shows that, although fixed at the dynamical stage, this observable cannot help in choosing the asystiffness of the EOS, because at each stage of the calculation the fragment multiplicities are located on the same straight line whether the asysoft or the asystiff EOS was used.

B. Preequilibrium emission

We define the multifragmenting source as the largest single cluster recognized by the clusterization algorithm at $t = 120$ fm/c, the rest of the system being considered as preequilibrium emission. As in Ref. [37] we find that the rate of nucleon emission in SMF is large between 60 and 120 fm/c and becomes constant at a small value afterwards; this is a general feature of all semiclassical transport models. The evolution of the number of preequilibrium nucleons (defined as the difference between numbers of neutrons or protons of the system and of the source) with the N/Z of the systems is shown in Fig. 6, for reactions at 45 A MeV. In all cases about 23% of the mass (charge) of the system has been emitted at 120 fm/c. The neutron-richest system has 24 extra neutrons compared to the neutron-poorest one; we observe that the former system ejected 8–9 more neutrons and 2 fewer protons. With an asysoft EOS, there are more neutrons and fewer protons emitted than in the asystiff case.

[2]The multiplicity of fragments with $Z \geqslant 3$ is, for all systems, larger after deexcitation than at 300 fm/c, which is not the case for that of fragments with $Z \geqslant 5$.

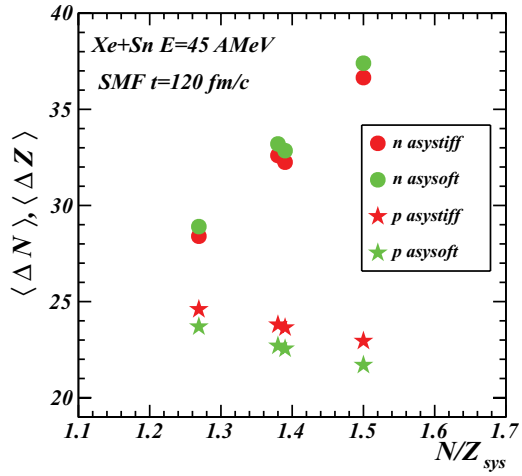

FIG. 6. (Color online) Average neutron (circles) and proton (stars) preequilibrium emission vs the N/Z of the total systems at 45 A MeV. The two points corresponding to $N/Z = 1.38$ have been shifted for visibility. Results are shown for the two asy-EOS.

In the model most of that emission occurs during the expansion of the system, and thus it is a witness of subnormal density EOS [37]; in that density region the symmetry potential is more repulsive for neutrons, and more attractive for protons in the asysoft case, which explains the relative values displayed in Fig. 6. Whatever the EOS is, in all cases the neutron-to-proton ratio of the fast emission is more neutron rich than the system for ^{136}Xe + ^{124}Sn, and more neutron poor for ^{124}Xe + ^{112}Sn. Consequently the isospin content of the multifragmenting sources is smaller than that of the total system for ^{136}Xe + ^{124}Sn, and larger for ^{124}Xe + ^{112}Sn, which reduces the N/Z range explored in multifragmentation. For the intermediate systems, the source is slightly more neutron-rich than the system with the asystiff EOS, and less for the asysoft EOS.

Isolating preequilibrium emission in experiments is a difficult task. A possible choice is to look at high-energy nucleons, possibly including nucleons bound in clusters [6,38]. We propose as an alternative to look at the complementary part of the proton preequilibrium emission, the "liquid phase," through the value of the total charge bound in fragments, $Z_{b_5} = \sum_1^{M_{\rm frag}} Z_{Z\geqslant 5}$. Obviously this variable is only meaningful provided that the detected events contain a large part of the total charge of the system, which is the case of our selected events. We want to test the dependence of Z_{b_5} on the symmetry energy term implemented in the simulations. In this aim we have followed the evolution of Z_{b_5} as a function of the collision stage, for the measured systems, and compared the final result of the calculations with the experimental data. We show in Table III the mean values and standard deviations of the experimental and calculated (primary, and cold before and after filtering) distributions for the different systems. We clearly observe that the experimental distributions are shifted upwards for the neutron-rich systems. In simulations the mean values of the distributions decrease whereas the standard deviations increase when going from primary to cold fragments and to the filtered distributions. The simulated mean values at all stages are, as in the experiment, larger when the system is more neutron rich. The filtered mean value agrees rather well with the experimental one for ^{124}Xe + ^{112}Sn, while it is more and more underestimated for the two other systems. We also notice that the filtered distributions are broader than the measured ones. We remark that the final calculated $\langle Z_{b_5}\rangle$ does not depend on the asystiffness of the EOS for the neutron-poor system whereas it becomes larger in the asysoft case when the system contains more neutrons.

If we compare the results for the extreme systems, ^{136}Xe + ^{124}Sn and ^{124}Xe + ^{112}Sn, the difference between the number of preequilibrium protons is negative (fourth column of Table III and Fig. 6). Therefore we expect a positive difference, ΔZ_{b_5}, when we turn to the values of Z_{b_5}, which is observed in the model for primary fragments at 300 fm/c, and for cold fragments. Note that the difference between the two systems grows larger during secondary decay, indicating that while it is essentially due to the first stage of the collision, part of it comes from the evaporation process. The filtering makes the ΔZ_{b_5} smaller again. At all steps the difference between the two systems is larger for the asysoft EOS. Experimentally we do observe a positive ΔZ_{b_5}, which is larger than what is obtained with any of the two EOS. The authors of Ref [37] underline that the calculated ΔZb_5 values depend on the fragment formation process; the spinodal decomposition which drives multifragmentation in SMF strongly disfavors the formation of light fragments as compared with an antisymmetrized molecular dynamics (AMD) calculation (see Fig. 8 of Ref. [37]). However, in view of the significant measured difference between the two systems, we think that ΔZ_{b_5} might be, in the future, a good observable for constraining the EOS.

C. Fragment kinetic energies

The calculated average kinetic energy of the final fragments at 45 A MeV is represented in Fig. 3. As in Ref. [32], we have added to the average kinetic energies a thermal term ($3T/2$) which is not contained in the calculation. One immediately observes that the model largely underestimates the measured energies. The underestimation of the energy of fragments produced through multifragmentation in central collisions seems to be a general drawback of semiclassical transport models. In Ref. [32], we found that in the BOB simulation the fragment kinetic energies were about 20% below the experimental values for ^{129}Xe + $^{\rm nat}$Sn at 32 A MeV. Several causes of the discrepancy were identified [22]: thermal fluctuations were reduced by the large number of test particles, whereas quantal fluctuations were neglected. Second, the finite range of the force introduced in the model was too large at normal density, creating surface energy at the detriment of fragment kinetic energy; the initial expansion energy was largely canceled. With the present SMF version the discrepancy between calculation and experiment reaches ∼40%. In this model the range of the force is correct for all densities; thermal fluctuations are still underestimated and in addition the large amount of preequilibrium emission considerably reduces the available energy of the fragmenting system. Indeed in

TABLE III. For the three systems studied at $E/A = 45$ MeV: mean experimental value of Z_{b_5}; for SMF simulations, and the two asy-EOS: number of protons lost at 120 fm/c, Z_{b_5} for primary fragments (at 300 fm/c), for cold fragments, and after filtering. In all cases the numbers between parentheses give the standard deviations of the corresponding distributions.

System	Exp.	SMF				
	$\langle Z_{b_5}\rangle$	asy	$\langle Z_{pr}\rangle$	$\langle Z_{b_5}^{prim}\rangle$	$\langle Z_{b_5}^{cold}\rangle$	$\langle Z_{b_5}^{filt}\rangle$
^{124}Xe + ^{112}Sn	41.9 (8.1)	stiff	24.60 (1.23)	63.2 (2.7)	47.2 (5.06)	41.6 (8.42)
		soft	23.72 (1.23)	63.9 (2.8)	47.4 (5.06)	41.6 (8.52)
^{136}Xe + ^{112}Sn	44.4 (8.1)	stiff	23.65 (1.21)	64.4 (2.8)	48.9 (5.21)	42.9 (8.72)
		soft	22.55 (1.12)	65.7 (2.6)	49.6 (5.17)	43.4 (8.90)
^{136}Xe + ^{124}Sn	46.2 (8.3)	stiff	22.95 (1.20)	65.2 (2.9)	49.8 (5.48)	43.4 (8.96)
		soft	21.71 (1.13)	66.6 (2.7)	50.6 (5.42)	44.0 (9.06)

Ref. [37] it is shown that the AMD model produces fewer preequilibrium nucleons, and fragments with larger kinetic energies. The overestimation of particle emission seems to be a rather general problem of semiclassical approaches, as is also stressed in Ref. [39]. However, it is interesting to note that in all simulations (BOB, SMF, AMD) for Sn+Sn or Xe+Sn collisions between 30 and 50 A MeV the excitation energy of the fragments is found close to 3 A MeV. The lack of available energy in SMF with respect to AMD thus only appears in the kinetic energy of the fragments. Finally, the isospin effect experimentally observed is not predicted by the calculation, which is not surprising if the effect comes from the expansion energy, which is consumed during the fragment formation.

Coming back to the results displayed in Table III, we notice that the values of Z_{b_5} from the filtered model and the experiment are similar, which would imply a correct number of nucleons emitted at 300 fm/c. We should, however, stress again that we could not apply the exact experimental selections to the calculation (completeness of the events) and that we used a simple geometrical filter.

V. SUMMARY AND CONCLUSIONS

We have studied central collisions between different isotopes of Xe and Sn nuclei, leading to systems differing by their number of neutrons, at incident energies of 32 and 45 A MeV. Experimentally we highlighted several isospin effects. At a given incident energy the lcp multiplicity decreases whereas the fragment multiplicity increases with the N/Z of the system. The stochastic mean field model developed in Catania well accounts for the fragment partition properties at 45 A MeV, while at 32 A MeV the model is not able to describe the multifragmentation process. Comparing model and experimental data, we infer that the increase of the fragment multiplicity essentially comes from the dynamical part of the reaction, but does not help in constraining the symmetry energy term of the EOS. Indeed this seems to be related just to the larger size of the fragmenting source in the neutron-richer cases.

We also found that on average the fragment kinetic energy grows larger when the isospin of the system increases, and we think that this observation confirms the existence of an expansion energy and shows that the primary fragments keep some sign of the neutron-richness of the initial system. The model fails in reproducing the fragment kinetic properties, one of the reasons being that too much energy is removed from the system by preequilibrium emission.

Finally, we propose to use the charge bound in fragments as an alternate variable to get information on lcp preequilibrium emission. We experimentally observe a sizable difference between the values of Z_{b_5} measured for ^{136}Xe + ^{124}Sn and ^{124}Xe + ^{112}Sn, which makes it a promising observable to constrain the symmetry energy. The calculated values of this difference depend on the asystiffness of the EOS, but are smaller than the measured one both in the asysoft and asystiff cases.

In prospective, further developments of stochastic transport models are in progress. Phase space fluctuations are introduced by a stochastic treatment of the nucleon-nucleon collision integral. Once a two-body collision occurs, two clouds of test particles, which simulate the wave-packet extension of the colliding nucleons, are moved simultaneously to new phase-space locations. This procedure, which corresponds to a numerical implementation of the Boltzmann-Langevin equation, has been proven to give the correct amplitude of equilibrium thermal fluctuations [40]. First tests with this model show an improvement of the description of the kinematical and partition properties of fragmenting systems in dissipative collisions around the Fermi energy [41].

[1] V. Baran, M. Colonna, V. Greco, and M. Di Toro, Phys. Rep. **410**, 335 (2005).
[2] Bao-An Li, Lie-Wen Chen, and Che Ming Ko, Phys. Rep. **464**, 113 (2008).
[3] M. F. Rivet, lecture given at the Joliot-Curie school, 2009 (unpublished), http://hal.in2p3.fr/in2p3-00584498.
[4] M. B. Tsang, T. X. Liu, L. Shi, P. Danielewicz, C. K. Gelbke, X. D. Liu, W. G. Lynch, W. P. Tan, G. Verde, A. Wagner, H. S. Xu, W. A. Friedman, L. Beaulieu, B. Davin, R. T. de Souza, Y. Larochelle, T. Lefort, R. Yanez, J. V. E. Viola, R. J. Charity, and L. G. Sobotka, Phys. Rev. Lett. **92**, 062701 (2004).
[5] L. W. Chen, C. M. Ko, and B. A. Li, Phys. Rev. Lett. **94**, 032701 (2005).
[6] Y. Zhang, P. Danielewicz, M. Famiano, Z. Li, W. G. Lynch, and M. B. Tsang, Phys. Lett. B **664**, 145 (2008).

[7] M. B. Tsang, Y. Zhang, P. Danielewicz, M. Famiano, Z. Li, W. G. Lynch, and A. W. Steiner, Phys. Rev. Lett. **102**, 122701 (2009).
[8] B. Borderie and M. F. Rivet, Prog. Part. Nucl. Phys. **61**, 551 (2008).
[9] J. Pouthas, B. Borderie, R. Dayras, E. Plagnol, M. F. Rivet, F. Saint-Laurent, J. C. Steckmeyer, G. Auger, C. O. Bacri, S. Barbey, A. Barbier, A. Benkirane, J. Benlliure, B. Berthier, E. Bougamont, P. Bourgault, P. Box, R. Bzyl, B. Cahan, Y. Cassagnou, D. Charlet, J. L. Charvet, A. Chbihi, T. Clerc, N. Copinet, D. Cussol, M. Engrand, J. M. Gautier, Y. Huguet, O. Jouniaux, J. L. Laville, P. Le Botlan, A. Leconte, R. Legrain, P. Lelong, M. Le Guay, L. Martina, C. Mazur, P. Mosrin, L. Olivier, J. P. Passerieux, S. Pierre, B. Piquet, E. Plaige, E. C. Pollaco, B. Raine, A. Richard, J. Ropert, C. Spitaels, L. Stab, D. Sznajderman, L. Tassan-Got, J. Tillier, M. Tripon, P. Vallerand, C. Volant, P. Volkov, J. P. Wieleczko, and G. Wittwer, Nucl. Instrum. Methods Phys. Res., Sect. A **357**, 418 (1995).
[10] F. Gagnon-Moisan, Ph.D. thesis, Université Paris XI Orsay et Université Laval Québec, 2010 (unpublished), http://tel.archives-ouvertes.fr/tel-00491182.
[11] J. Moisan, Ph.D. thesis, Université de Caen et Université Laval Québec, 2008 (unpublished), http://tel.archives-ouvertes.fr/tel-00336062.
[12] G. Schiwietz and P. L. Grande, Nucl. Instrum. Methods B **175**, 125 (2001).
[13] S. Kox, A. Gamp, R. Cherkaoui, A. J. Cole, N. Longequeue, J. Menet, C. Perrin, and J. B. Viano, Nucl. Phys. A **420**, 162 (1984).
[14] J. D. Frankland, C. O. Bacri, B. Borderie, M. F. Rivet, M. Squalli, G. Auger, N. Bellaize, F. Bocage, R. Bougault, R. Brou, P. Buchet, A. Chbihi, J. Colin, D. Cussol, R. Dayras, A. Demeyer, D. Doré, D. Durand, E. Galichet, E. Genouin-Duhamel, E. Gerlic, D. Guinet, P. Lautesse, J. L. Laville, J. F. Lecolley, R. Legrain, N. Le Neindre, O. Lopez, M. Louvel, A. M. Maskay, L. Nalpas, A. D. Nguyen, M. Pârlog, J. Péter, E. Plagnol, E. Rosato, F. Saint-Laurent, S. Salou, J. C. Steckmeyer, M. Stern, G. Tăbăcaru, B. Tamain, O. Tirel, L. Tassan-Got, E. Vient, C. Volant, and J. Wieleczko (INDRA Collaboration), Nucl. Phys. A **689**, 905 (2001).
[15] S. Hudan, A. Chbihi, J. D. Frankland, A. Mignon, A. Botvina, J. P. Wieleczko, G. Auger, N. Bellaize, B. Borderie, R. Bougault, B. Bouriquet, A. M. Buta, J. Colin, D. Cussol, R. Dayras, A. Demeyer, D. Durand, E. Galichet, D. Guinet, B. Guiot, G. Lanzalone, P. Lautesse, F. Lavaud, J. F. Lecolley, R. Legrain, N. Le Neindre, O. Lopez, L. Manduci, J. Marie, L. Nalpas, J. Normand, M. Pârlog, P. Pawłowski, E. Plagnol, M. F. Rivet, E. Rosato, R. Roy, J. C. Steckmeyer, G. Tăbăcaru, B. Tamain, A. van Lauwe, E. Vient, M. Vigilante, and C. Volant (INDRA Collaboration), Phys. Rev. C **67**, 064613 (2003).
[16] G. Tăbăcaru, B. Borderie, P. Désesquelles, M. Pârlog, M. F. Rivet, R. Bougault, B. Bouriquet, A. M. Buta, E. Galichet, B. Guiot, P. Lautesse, N. Le Neindre, L. Manduci, E. Rosato, B. Tamain, M. Vigilante, and J. P. Wieleczko, Eur. Phys. J. A **18**, 103 (2003).
[17] G. Tăbăcaru, M. F. Rivet, B. Borderie, M. Pârlog, B. Bouriquet, A. Chbihi, J. D. Frankland, J. P. Wieleczko, E. Bonnet, R. Bougault, R. Dayras, E. Galichet, D. Guinet, P. Lautesse, N. Le Neindre, O. Lopez, L. Manduci, L. Nalpas, P. Pawłowski, E. Rosato, R. Roy, S. Salou, B. Tamain, E. Vient, M. Vigilante, and C. Volant (INDRA Collaboration), Nucl. Phys. A **764**, 371 (2006).
[18] S. Salou, Ph.D. thesis, Université de Caen, 1997 (ubpublished), http://tel.archives-ouvertes.fr/tel-00003688.
[19] J. F. Dempsey, R. J. Charity, L. G. Sobotka, G. J. Kunde, S. Gaff, C. K. Gelbke, T. Glasmacher, M. J. Huang, R. C. Lemmon, W. G. Lynch, L. Manduci, L. Martin, M. B. Tsang, D. K. Agnihotri, B. Djerroud, W. U. Schröder, W. Skulski, J. Tõke, and W. A. Friedman, Phys. Rev. C **54**, 1710 (1996).
[20] G. J. Kunde, S. Gaff, C. K. Gelbke, T. Glasmacher, M. J. Huang, R. C. Lemmon, W. G. Lynch, L. Manduci, L. Martin, M. B. Tsang, W. A. Friedman, J. F. Dempsey, R. J. Charity, L. G. Sobotka, D. K. Agnihotri, B. Djerroud, W. U. Schröder, W. Skulski, J. Tõke, and K. Wyrozebski, Phys. Rev. Lett. **77**, 2897 (1996).
[21] W. A. Friedman, Phys. Rev. C **42**, 667 (1990).
[22] M. F. Rivet, C. O. Bacri, B. Borderie, J. D. Frankland, M. Assenard, G. Auger, F. Bocage, R. Bougault, R. Brou, P. Buchet, A. Chbihi, J. Colin, R. Dayras, A. Demeyer, D. Doré, D. Durand, P. Eudes, E. Galichet, E. Genouin-Duhamel, E. Gerlic, M. Germain, D. Guinet, P. Lautesse, J. L. Laville, J. F. Lecolley, A. Le Fèvre, T. Lefort, R. Legrain, N. Le Neindre, O. Lopez, M. Louvel, L. Nalpas, A. D. Nguyen, M. Pârlog, J. Péter, E. Plagnol, A. Rahmani, T. Reposeur, E. Rosato, F. Saint-Laurent, S. Salou, M. Squalli, J. C. Steckmeyer, M. Stern, G. Tăbăcaru, B. Tamain, L. Tassan-Got, O. Tirel, D. Vintache, C. Volant, J. P. Wieleczko, A. Guarnera, M. Colonna, and P. Chomaz (INDRA Collaboration), Phys. Lett. B **430**, 217 (1998).
[23] N. Marie, R. Laforest, R. Bougault, J. P. Wieleczko, D. Durand, C. O. Bacri, J. F. Lecolley, F. Saint-Laurent, G. Auger, J. Benlliure, E. Bisquer, B. Borderie, R. Brou, J. L. Charvet, A. Chbihi, J. Colin, D. Cussol, R. Dayras, E. De Filippo, A. Demeyer, D. Doré, P. Ecomard, P. Eudes, D. Gourio, D. Guinet, P. Lautesse, J. L. Laville, A. Le Fèvre, T. Lefort, R. Legrain, O. Lopez, M. Louvel, V. Métivier, L. Nalpas, A. Ouatizerga, M. Pârlog, J. Péter, E. Plagnol, A. Rahmani, T. Reposeur, M. F. Rivet, E. Rosato, S. Salou, M. Squalli, J. C. Steckmeyer, B. Tamain, L. Tassan-Got, E. Vient, and C. Volant (INDRA Collaboration), Phys. Lett. B **391**, 15 (1997).
[24] W. Hsi, G. J. Kunde, J. Pochodzalla, W. G. Lynch, M. B. Tsang, M. L. Begemann-Blaich, D. R. Bowman, R. J. Charity, F. Cosmo, A. Ferrero, C. K. Gelbke, T. Glasmacher, T. Hofmann, G. Imme, I. Iori, J. Hubele, J. Kempter, P. Kreutz, W. D. Kunze, V. Lindenstruth, M. A. Lisa, U. Lynen, M. Mang, A. Moroni, W. F. J. Müller, M. Neumann, B. Ocker, C. A. Ogilvie, G. F. Peaslee, G. Raciti, F. Rosenberger, H. Sann, R. S. A. Schüttauf, C. Schwarz, W. Seidel, V. Serfling, L. G. Sobotka, L. Stuttge, S. Tomasevic, W. Trautmann, A. Tucholski, C. Williams, A. Wörner, and B. Zwieglinski, Phys. Rev. Lett. **73**, 3367 (1994).
[25] D. Durand, Nucl. Phys. A **654**, 273c (1999).
[26] B. Tamain, in *Dynamics and Thermodynamics with Nuclear Degrees of Freedom*, Eur. Phys. J. A, Vol. 30, edited by P. Chomaz, F. Gulminelli, W. Trautmann, and S. J. Yennello (Springer, Berlin, 2006), pp. 71–79.
[27] A. R. Raduta, B. Borderie, E. Bonnet, N. Le Neindre, S. Piantelli, and M. F. Rivet, Phys. Lett. B **623**, 43 (2005).
[28] I. Lombardo, C. Agodi, F. Amorini, A. Anzalone, L. Auditore, I. Berceanu, G. Cardella, S. Cavallaro, M. B. Chatterjee, E. De Filippo, E. Geraci, G. Giuliani, L. Grassi, J. Han, E. L. Guidara, D. Loria, G. Lanzalone, C. Maiolino, A. Pagano, M. Papa, S.

Pirrone, G. Politi, F. Porto, F. Rizzo, P. Russotto, A. Trifirò, M. Trimarchi, G. Verde, and M. Vigilante, Phys. Rev. C **84**, 024613 (2011).

[29] M. Colonna, M. Di Toro, A. Guarnera, S. Maccarone, M. Zielinska-Pfabé, and H. H. Wolter, Nucl. Phys. A **642**, 449 (1998).

[30] E. Galichet, M. Colonna, B. Borderie, and M. F. Rivet, Phys. Rev. C **79**, 064615 (2009).

[31] A. Guarnera, M. Colonna, and P. Chomaz, Phys. Lett. B **373**, 267 (1996).

[32] J. D. Frankland, B. Borderie, M. Colonna, M. F. Rivet, C. O. Bacri, P. Chomaz, D. Durand, A. Guarnera, M. Pârlog, M. Squalli, G. Tăbăcaru, G. Auger, N. Bellaize, F. Bocage, R. Bougault, R. Brou, P. Buchet, A. Chbihi, J. Colin, D. Cussol, R. Dayras, A. Demeyer, D. Doré, E. Galichet, E. Genouin-Duhamel, E. Gerlic, D. Guinet, P. Lautesse, J. L. Laville, J. F. Lecolley, R. Legrain, N. Le Neindre, O. Lopez, M. Louvel, A. M. Maskay, L. Nalpas, A. D. Nguyen, E. Plagnol, E. Rosato, F. Saint-Laurent, S. Salou, J. C. Steckmeyer, B. Tamain, L. Tassan-Got, O. Tirel, E. Vient, C. Volant, and J. Wieleczko (INDRA Collaboration), Nucl. Phys. A **689**, 940 (2001).

[33] D. Durand, Nucl. Phys. A **541**, 266 (1992).

[34] S. Piantelli, B. Borderie, E. Bonnet, N. Le Neindre, A. R. Raduta, M. F. Rivet, R. Bougault, A. Chbihi, R. Dayras, J. D. Frankland, E. Galichet, F. Gagnon-Moisan, D. Guinet, P. Lautesse, G. Lehaut, O. Lopez, D. Mercier, J. Moisan, M. Pârlog, E. Rosato, R. Roy, B. Tamain, E. Vient, M. Vigilante, and J. P. Wieleczko (INDRA Collaboration), Nucl. Phys. A **809**, 111 (2008).

[35] P. Napolitani, M. Colonna, F. Gulminelli, E. Galichet, S. Piantelli, G. Verde, and E. Vient, Phys. Rev. C **81**, 044619 (2010).

[36] E. Galichet, M. F. Rivet, F. Gagnon-Moisan, B. Borderie, M. Colonna, and R. Roy (INDRA Collaboration), in *Proceedings of the International Workshop on Multifragmentation and Related Topics 2011, Caen, France*, edited by J. D. Frankland, A. Pagano, S. Pirrone, M. F. Rivet, and F. Rizzo (SIF, Bologna, 2012), p. 131, http://dx.doi.org/10.1051/epjconf/20123100017.

[37] M. Colonna, A. Ono, and J. Rizzo, Phys. Rev. C **82**, 054613 (2010).

[38] P. Sapienza, R. Coniglione, M. Colonna, E. Migneco, C. Agodi, R. Alba, G. Bellia, A. Del Zoppo, P. Finocchiaro, V. Greco, K. Loukachine, C. Maiolino, P. Piattelli, D. Santonocito, P. G. Ventura, Y. Blumenfeld, M. Bruno, N. Colonna, M. D'Agostino, L. Fabbietti, M. L. Fiandri, F. Gramegna, I. Iori, G. Margagliotti, P. F. Mastinu, P. M. Milazzo, A. Moroni, R. Rui, J. A. Scarpaci, and G. Vannini, Phys. Rev. Lett. **87**, 072701 (2001).

[39] D. Lacroix and P. Chomaz, Nucl. Phys. A **636**, 85 (1998).

[40] J. Rizzo, P. Chomaz, and M. Colonna, Nucl. Phys. A **806**, 40 (2008).

[41] P. Napolitani and M. Colonna, in *Proceedings of the International Workshop on Multifragmentation and Related Topics 2011, Caen, France*, edited by J. D. Frankland, A. Pagano, S. Pirrone, M. F. Rivet, and F. Rizzo (SIF, Bologna, 2012), p. 205, http://dx.doi.org/10.1051/epjconf/20123100027.